CSM Instruments
Advanced Mechanical Surface Testing

APPLICATIONS BULLETIN

Forthcoming Nano Scratch Tester (NST) for characterisation of ultra-thin films

Introduction

This application note focusses on a new scratch testing instrument currently being developed at CSEM Instruments. With the everdecreasing thicknesses of industrial coatings and films has emerged a significant demand for an ultra-high resolution scratch testing apparatus capable of accurately characterising such materials. Examples of domains where this technology can be readily demonstrated include the thin DLC overcoats used in the magnetic hard disk industry and varnish clearcoats used in the automobile industry.

The prototype Nano Scratch Tester (NST) is designed to exploit the normal force range from 10 mN to 1 N, this being achieved by using three interchangeable cantilevers of varying stiffness to apply the required load range. The tip is mounted on the cantilever and deflection is measured by a Linear Voltage Differential Transformer (LVDT).

Owing to the small size of the scratched path, it is not always easy to distinguish interesting features under a conventional optical microscope, due to lack of resolution. One solution is to profile the scratched area with a stylus profilometer, but in certain cases (especially soft materials such as polymers) this can significantly damage the sample. The NST incorporates a standard optical microscope, but has the additional option of an integrated scanning force microscope (SFM) objective, as described in Bulletin No. 3 (May 1997). This permits high resolution imaging of a scratched area and quantitative measurement of lateral and depth dimensions. In addition, surface morphology can be investigated before scratching.

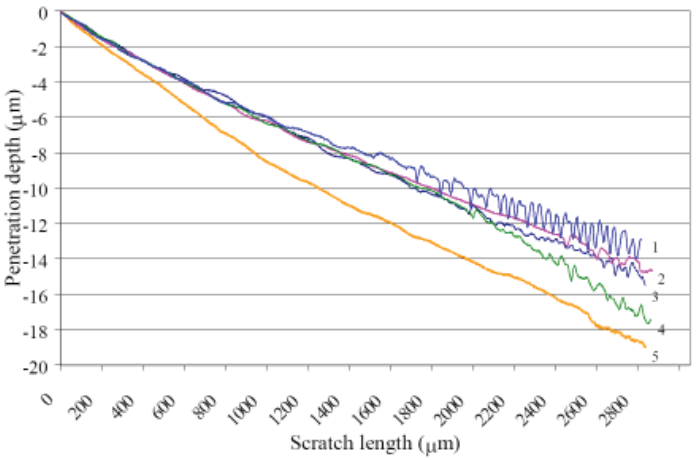

Figure 1: Penetration depth plotted as a function of scratch length for five polymeric varnish overcoats of varying mar resistance.

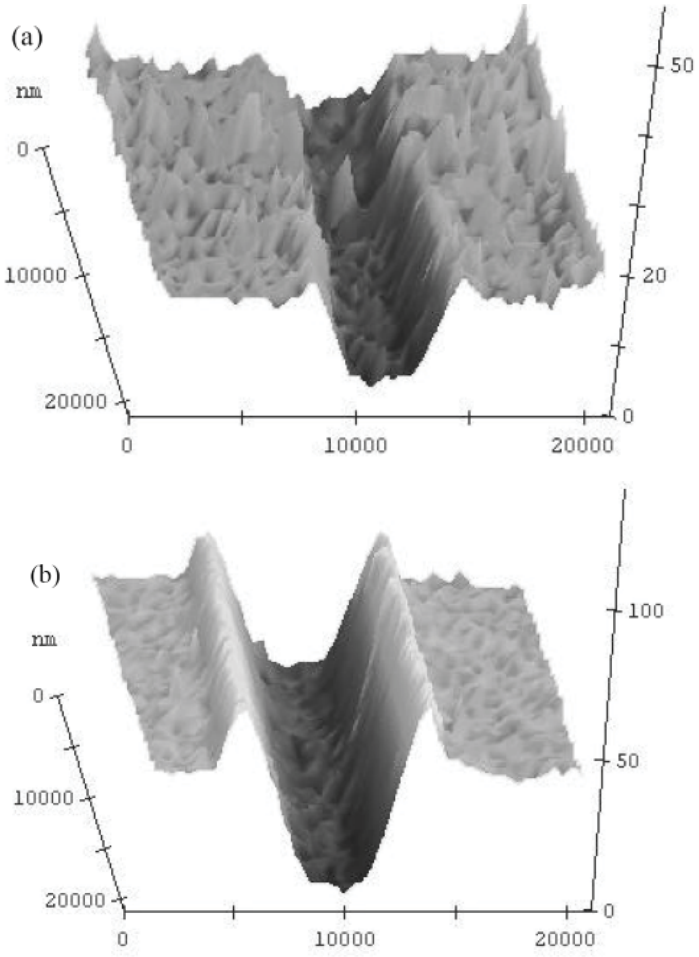

Figure 2 : Three-dimensional SFM images of scratches made on polymeric varnish overcoats. It is clear that low applied loads (a) produce less plastic deformation than higher loads (b).

Applications

A selection of five different automotive clearcoat varnish samples were obtained from Cytec Industries Inc., a company which supplies crosslinking additives to automotive coating manufacturers. These samples were selected to give a wide range of mar resistance, i.e., the ability of the coating to resist damage caused by light abrasion. The difference between mar and scratch resistance is that mar is related only to the relatively fine surface scratches which spoil the appearance of an automotive coating.

The NST is therefore ideally suited to simulating such scratch damage in a controlled way, for example, damage caused in service due to car washing, polishing, grit impact, or other environmental conditions. A quantitative description of these effects is usually given in terms of gloss reduction, increase in haze or shift in grey level. Haze measurements can also reveal the anisotropy of the scratch direction.

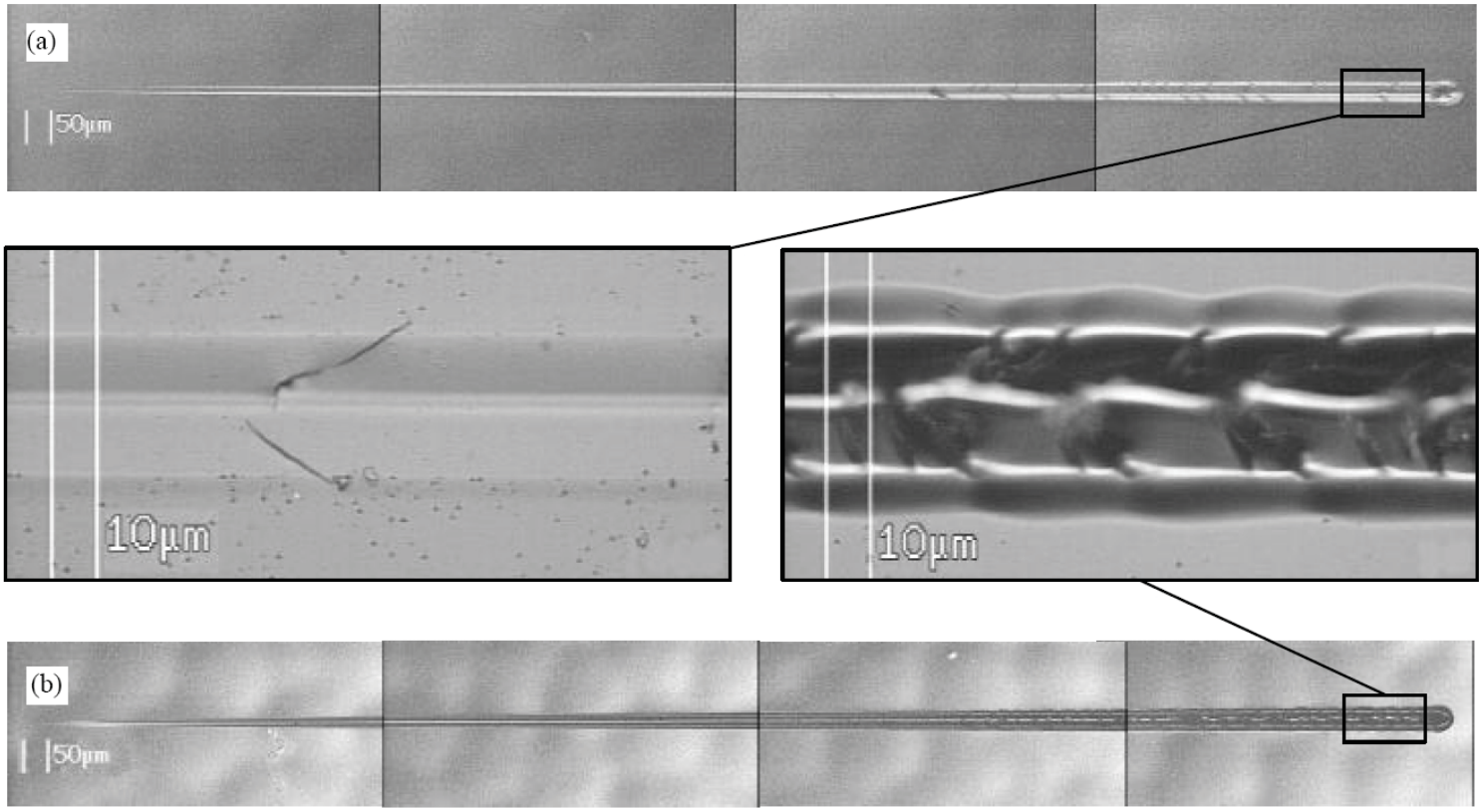

Fig 3 : Optical micrographs of scratch paths made over the same progressive load range (0 - 200 mN) on two different polymeric overcoats. The high resolution close-up images show the significant difference between a coating which exhibits a good mar resistance (a) and one which has poor mar resistance characterised by plastic deformation (b).

The five measured samples are summarised in Table 1 with their known mar resistance ratings. Five progressive normal load scratches were performed on each sample and average values taken for the two critical loads, Lc1 and Lc2. The load range used was 0 - 200 mN, sliding speed 50mm/s and scratch length 2.8 mm. The diamond stylus used had a tip radius of 10mm.

Fig. 1 summarises the evolution of penetration depth for a scratch made on each of the five samples and it is evident that the coatings exhibiting good mar resistance have a greater depth but a much smoother depth profile. The less mar-resistant coatings have an increasingly rough profile after the applied load has exceeded the first critical point, Lc1. Such phenomena are confirmed by subsequent optical microscopy, as depicted in Fig. 3. By photographing the scratch in sections it is possible to recreate the entire path and then zoom-in on particular areas of interest. The high resolution close-up images show the significant difference between a coating which exhibits an excellent mar resistance (Fig. 3 (a)) and one which has poor mar resistance characterised by plastic deformation (Fig. 3 (b)).

Sample N°.	Mar resistance	L_c1	L_c2
1	Poor	81	123
2	Poor	59	107
3	Moderate	94	129
4	Good	88	160
5	Excellent	94	173

Fig 3 : Summary of the five tested varnish samples, together with their measured values of critical load Lc1 (first lateral cracking) and Lc2 (first severe cracking and delamination).

Although such deformation can be seen with an optical microscope, it cannot be quantitatively measured. For this reason, the integrated SFM objective is utilised to measure selected sections of a scratch and accurately determine the extent of pile-up along its edges, cracking in and around the scratch path and other plastic or brittle deformation behaviour. Two such examples are shown in Fig. 2 for images made near the beginning (a) and end (b) of a typical scratch. Clearly, at low applied loads, plastic deformation is restricted whereas at higher loads the formation of pile-up material on either side of the advancing indenter becomes significant.

The prototype NST has been shown to satisfy a distinct need among manufacturers of ultra-thin and soft polymeric coatings. With the addition of an integrated SFM, this instrument promises to be a unique tool for the more complete characterisation of thin films in many other sectors of research and industry.

Microstructured silicon wafers compared with the CSM Tribometer

Introduction

A new concept in the field of tribology has been the development of material surfaces which are designed specifically for improved lubrication capability. These can vary from simple control of the surface roughness of two mating surfaces, to the more complex formation of regular structures which serve the double purpose of retaining lubricant and trapping debris particles. This application note presents some results of Tribometer tests on microstructured silicon wafers having regularly spaced, square-shaped pits of varying dimensions.

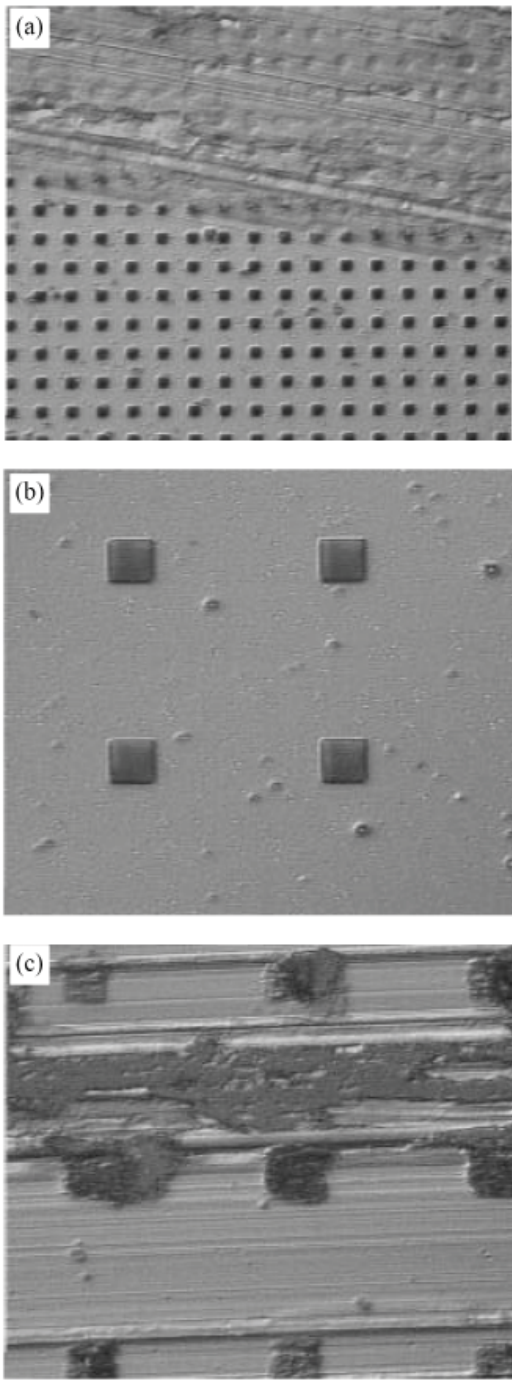

Fig 1 : Optical micrographs of a typical microstructured silicon sur face (a) at edge of wear track, (b) before testing, and (c) after testing where debris and scratches are clearly visible.

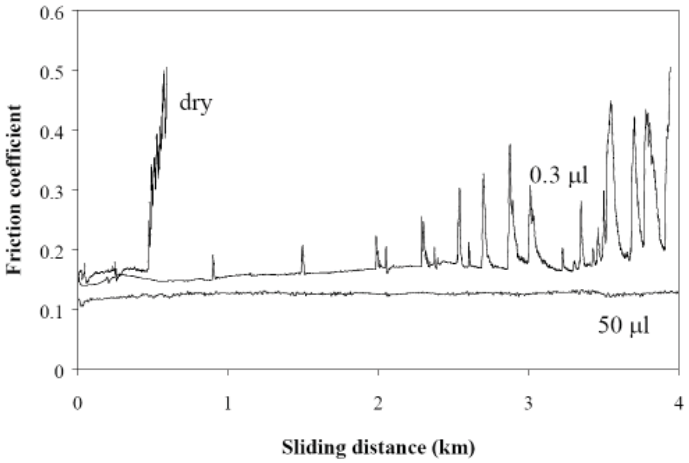

Fig 2 : Friction traces obtained on a typical microstructured silicon surface. Note the drastic improvement in wear life when the system is lubricated.

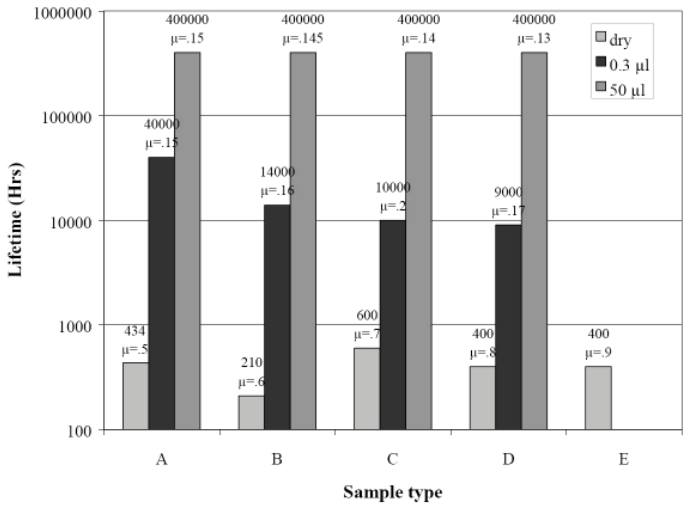

Fig 3 : Summarised results for four microstructured samples (A to D) and a smooth sample (E) under dry and lubricated conditions.

Application

A ball-on-disk pair was chosen (ball Æ = 6 mm) with an applied load of 5 N, a sliding speed of 0.1 ms-1 and standard laboratory conditions (22°C, 50% RH). The samples were tested under dry, lightly lubricated (0.3 µl) and heavily lubricated (50 µl) conditions and the oil used was a standard synthetic grade. The results in Figs 2 and 3 confirm the effectiveness of microstructure control in extending service life, especially under boundary and/or hydrodynamic lubrication conditions. Unlubricated conditions cause a rapid decline in wear life, whereas good lubrication ensures smooth operation over a large number of cycles. An underlying trend seems to be that under lightly lubricated conditions, a reduction in size of each pit' increases the overall lifetime of the system. This is most probably due to the lubricant molecules being more suited to capillary motion when a certain pit size is available to them, although further work is required in order to investigate such effects. A good correlation between molecule size and pit geometry is essential in providing optimum lubricated conditions.

Dr. M. Op de Hipt of the CSEM Tribo Coatings group is acknowledged for providing the presented data.

Combined NHT/SFM for investigating the tip defect of common indenters

Introduction

Apart from imaging the residual imprint of an indentation, the integrated SFM which is mounted on the NHT can also be used to check and quantify the tip defect and symmetry of the indenter used. The actual indenter tip, being fused to a vertical rod, can easily be removed from the NHT measuring head and positioned accurately under the SFM objective.

It has been shown [1] that the tip defect of common indenters can be significant, especially in the case of the Vickers geometry, owing to the difficulties in grinding a square-based pyramid to an adequate tip. In contrast, the three-sided pyramidal geometry of the Berkovich naturally terminates at a point, thus facilitating the grinding of diamonds which maintain their sharpness to very small scales. Berkovich tip defects, as characterised by the effective tip radius, are frequently less than 50 nm in many of the better diamonds.

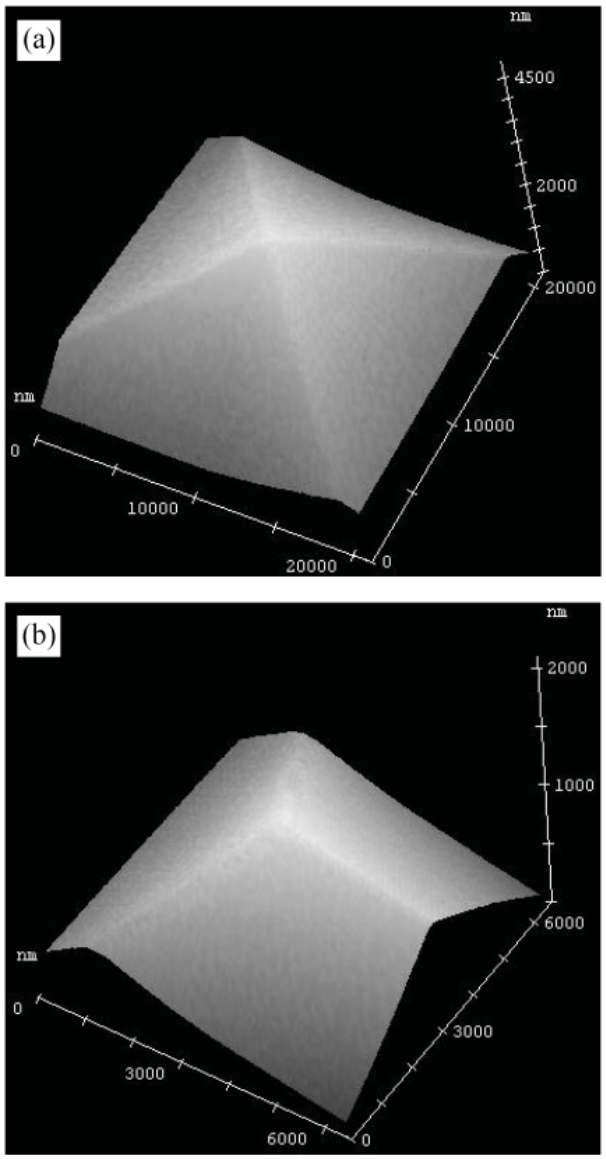

Fig 1 : Scanning force microscopy images of Vickers (a) and Berkovich (b) diamond indenters.

Application

Fig. 1 shows two SFM images of a Vickers and a Berkovich indenter. Although the SFM has a limited vertical range, most nanoindentations are less than 5 mm in depth, so the instrument is well suited to the measurement of the active portion of the indenter. In addition, the high resolution of the SFM allows shape information to be extracted directly from the images, as well as any deviation from a perfectly sharp pyramidal geometry. Previous work in this domain [2] has shown that the area function of a pyramidal indenter can be directly calculated from information gained from an SFM image, after correcting for the effects of pixellation and SFM probe shape.

Pixellation occurs due to the fact that SFM data are acquired in digital form and so have a finite number of data points. For example, for a lateral scan size of 20 mm, and using the maximum number of points per line (512), the separation between each data point will be 20000/512 = 39 nm. This means that an image of a typical pyramidal indenter will in fact be made up of steps of lateral separation 39 nm. If the contact area is to be calculated from such data then this may produce significant error, and so various correction routines must be used. Obviously, this effect is also present in SFM images of residual imprints and should be taken into account if pile-up volumes or contact areas are to be calculated.

[1] N. X. Randall, Development and application of a multifunctional nanotribological tool, PhD Thesis, University of Neuchâtel, Switzerland, 1997

[2] N. M. Jennet, G. Shafirstein and S. Saunders in 'Comparison of indenter tip shape measurement using a calibrated AFM and indentation into fused silica', Proc. Of the 9th Int. Symposium on Hardness Testing in Theory and Practice, Dusseldorf, 1995
(Publ. VDI-Verlag GmbH, Vol. 1194, 201-210)

csm Instruments

This Applications Bulletin is published quarterly and features interesting studies, new developments and other applications for our full range of mechanical surface testing instruments.

Editor Dr. Nicholas Randall

Should you require further information, then please contact:

CSM Instruments
Rue de la Gare 4
CH-2034 Peseux
Switzerland

Tel: + 41 32 557 5600
Fax: +41 32 557 5610
info@csm-instruments.com
www.csm-instruments.com

DISTRIBUTOR:

6210.04.98V1 CSM Instruments / Printed in Switzerland